Few-Body Syst (2024) 65:44
https://doi.org/10.1007/s00601-024-01911-7

Roman Skibiński · Henryk Witała · Jacek Golak

Impact of the N^4LO Short-Range Three-Nucleon Force Components on the Nucleon-Deuteron Spin Correlation Coefficients

Received: 21 January 2024 / Accepted: 14 March 2024
© The Author(s) 2024

Abstract The spin correlation coefficients in the neutron-deuteron elastic scattering process at incoming neutron laboratory energies E = 10, 135, 190, and 250 MeV are determined by solving the momentum space three-nucleon (3N) Faddeev equations. The chiral two-nucleon (2N) interaction with momentum-space semi-local (SMS) regularization up to the fifth order of chiral expansion (N^4LO), supplemented by the F-waves terms from the sixth order (N^5LO), is used. Additionally, the consistent 3N force (3NF) at the third order of chiral expansion, supplemented by the short-range contributions from N^4LO is applied. As a results, we give predictions for the complete set of spin correlation coefficients $C_{\alpha,\beta}$. We find that the effect of the investigated three-nucleon N^4LO components amounts up to several dozen percent, depending on reaction energy, scattering angle and type of spin correlation coefficient itself. Our results can serve as a guide for future measurements of the spin correlation coefficients.

1 Introduction

The last thirty years have been a period of many discoveries in the study of nuclear potentials and several-body processes. First, the new generation of semi-phenomenological potentials, such as the Argonne V18 [1] force or the CD Bonn [2] interaction, led to a significant improvement in the description of experimental data. This situation was further improved thanks to nuclear potential models derived from the Chiral Effective Field Theory. The most important advantages of the latter include (a) direct connection to QCD and other processes, like pion-nucleon scattering, (b) the possibility of deriving nuclear forces in a perturbative expansion, which allows assigning a physical sub-process to a specific order of expansion, (c) the possibility of deriving consistent two-nucleon, three-nucleon forces, etc. and (d) the hierarchy of nuclear forces naturally resulting from the model, justifying the treatment of many-body forces as corrections to the dominant two-nucleon interaction. Theoretical work has resulted in several chiral models of nuclear forces [3–16]. Among them, the results obtained by E. Epelbaum's group occupy a special place. This group has, over the years, provided several chiral force models, the most recent of which is the SMS model that uses the semi-local regularization. Within this model, complete two-body forces up to the fifth order of chiral expansion (N^4LO) have been derived to

R. Skibiński (✉)· H. Witała · J. Golak
Faculty of Physics, Astronomy and Applied Computer Science, Jagiellonian University, St. Łojasiewicza 11, 30348 Kraków, Poland
E-mail: roman.skibinski@uj.edu.pl

H. Witała
E-mail: henryk.witala@uj.edu.pl

J. Golak
E-mail: jacek.golak@uj.edu.pl

Published online: 15 April 2024

date. Further, some F-wave contributions from the next order are also known, and combined with the N^{4}LO SMS potential create the N^{4}LO$^+$ version of the model. That version of the interaction gives remarkably high quality of the two-nucleon data description, what can be quantified by χ^2/data ≈ 1.06 for neutron-proton data in the energy range 0–300 MeV [10].

On the other hand, the work of experimenters provides increasingly more accurate experimental results, facilitating verification of theoretical models. In the three-nucleon sector, very precise data are currently available for the cross-sections in elastic nucleon-deuteron scattering and in the deuteron breakup reaction induced by a nucleon [17–20]. The latter has been measured practically over the entire range of angles defining the momenta of free nucleons in the final state. These cross section data are accompanied by results for a number of polarization observables, with dominating measurements of the analyzing powers, i.e. for reactions with one polarized particle in the initial channel, see e.g. [21,22]. Some efforts were also made to measure more complex polarization observables, which resulted in, among others, experiments performed at the IUCF at energies of 135 and 200 MeV [23]. Due to the fact that the correct description of polarization observables is a more demanding task than the description of cross sections, further experiments in this field are currently planned. One of them is the spin correlation coefficients experiment planned at RIKEN [24,25].

With this in mind, in the present work we focus on theoretical predictions describing the impact of the short-range N^{4}LO three-nucleon force on a complete set of spin correlation coefficients. To present a systematic picture, we show results for five reaction energies, that is for five neutron kinetic energies in the laboratory frame. In following we stick to the nonrelativistic formalism, described in Sect. 2. Our results are given in Sect. 3 and we conclude in Sect. 4.

2 Formalism

In order to obtain the spin correlation coefficients a two-step procedure has been applied. First, the 13 free parameters of the 3NF have been found. They are c_D and c_E which occur at N^{2}LO and c_i, $i = 1, \ldots, 11$, present in the N^{4}LO short-range 3NF. To this end the emulator [26–28] was used to effectively perform the χ^2/data minimization fit, which in turn allowed us to prepare combined 3NF at N^{2}LO and N^{4}LO. In the second step, the obtained forces were used to solve the Faddeev equation, which enabled the determination of the transition amplitudes and observables [29]. Both the emulator and the solution of the full Faddeev equation were performed in momentum space and, in fact, were done within the same formalism.

The above-mentioned emulator is dedicated to the problem of adjusting the free parameters of the three-body force. It bases on several observations that allow us to introduce approximations to the Faddev's equations. Namely, we take advantage of the fact that the 3NF components associated with free parameters act only in the few lowest partial waves. Additionally, as described below, the second-order terms in the iterative equation can be neglected.

The starting point for the emulator used is the observation that the $V^{(1)}$ part of a 3NF, that is the part of 3NF symmetric under the exchange of particles 2 and 3, can be written as

$$V^{(1)} = V(\theta_0) + \sum_{i=1}^{N} c_i \Delta V_i \equiv V(\theta_0) + \Delta V(\theta) \;, \tag{1}$$

with a parameter-free term $V(\theta_0)$ and a sum of N parameter-dependent terms ΔV_i multiplied by strengths parameters c_i, collected in the $\Delta V(\theta)$ term.

If all the c_i parameters are known and full 3N Hamiltonian $H = H_0 + V^{2N} + V^{3N}$ does not contain any unknown parameters, one can proceed to the exact solution of the Faddeev equation

$$\begin{aligned} T|\phi\rangle &= tP|\phi\rangle + (1 + tG_0)V^{(1)}(1 + P)|\phi\rangle + tPG_0T|\phi\rangle \\ &\quad + (1 + tG_0)V^{(1)}(1 + P)G_0T|\phi\rangle \;, \end{aligned} \tag{2}$$

where G_0 is the free three-nucleon propagator, t is a solution of the Lippmann-Schwinger equation with the 2N potential V^{2N}, and P is a permutation operator. The initial state $|\phi\rangle \equiv |\mathbf{q}_0\rangle|\phi_d\rangle$ describes the free motion of the nucleon (neutron) with the relative momentum $\mathbf{q}_0$ and the internal deuteron wave function $|\phi_d\rangle$. The elastic scattering transition amplitude leading to the final neutron-deuteron state $|\phi'\rangle$ is then given by [29,30]

$$\langle\phi'|U|\phi\rangle = \langle\phi'|PG_0^{-1}|\phi\rangle + \langle\phi'|V^{(1)}(1 + P)|\phi\rangle$$

$$+\langle\phi'|V^{(1)}(1+P)G_0T|\phi\rangle + \langle\phi'|PT|\phi\rangle \; . \tag{3}$$

However, if the c_i parameters are unknown, one must first determine their values. We used the emulator [26–28] for this purpose. The splitting in (1) entails a similar splitting for the T operator $T = T(\theta_0)+\sum_{i=1}^{N} c_i \Delta T_i \equiv T(\theta_0) + \Delta T(\theta)$. Inserting both sums in the Faddeev equation (2) and neglecting, due to the smallness of the $\Delta V(\theta)$, the second-order terms, i.e. terms proportional to $\Delta V(\theta)(1+P)G_0\Delta T(\theta)$ allows us to end with a sequence of equations to be solved: one standard Faddeev equation for $T(\theta_0)$ dependent on $V(\theta_0)$ only, and N equations for ΔT_i, each of which depends only on one term ΔV_i and the parameter-free $V(\theta_0)$ part of 3NF. A few further steps, discussed in [27,28] lead to the elastic scattering amplitude. Its dependence on the c_i parameters is following:

$$\langle\phi'|U|\phi\rangle = \langle\phi'|U_0|\phi\rangle + \sum_i c_i \langle\phi'|U_i|\phi\rangle + \sum_{i,k} c_i c_k \langle\phi'|U_{ik}|\phi\rangle \; , \tag{4}$$

and is a convenient relation for practical use in χ^2/data minimization. In Eq. 4, the U_0, U_i, and U_{ik} are parts of the transition amplitude which depend neither on ΔV_i nor on ΔT_i, depend on ΔV_i or ΔT_i, or depend on ΔV_i and ΔT_i, respectively. The quality of this approximation was tested in [27], where it was shown that it is sufficient to realistically estimate the c_i values.

The fitting procedure was performed using a set of 786 data points, see Tab.2 of [28] at energies E = 10, 70 and 135 MeV. The resulting values of c_i parameters are given in Tab.3 of [28] and are also used to obtain the results presented in the next section. Note, that the two free parameters, of the N^{2}LO 3NF, c_D and c_E, have been fixed separately for calculations which take or do not take the short-range N^{4}LO 3NF into account.

We solve Eqs. (2) and (3) in the momentum-space partial-wave basis $|pq\alpha\rangle$, defined by the magnitudes of the relative Jacobi momenta p and q and a set of discrete quantum numbers α comprising angular momenta, spins and isospins in the j-I coupling. We take into account all the 3N partial wave states up to the 2N angular momentum $j_{max} = 5$ and the 3N angular momentum $J_{max} = \frac{25}{2}$. We restrict the 3NF to act in the partial waves with the total 3N angular momentum $J \leq 7/2$. For details of our numerical performance see [29].

3 Results

There are 13 non-zero spin correlation coefficients [29], with the deuteron being in vector or tensor polarization state. In the following we stick to the standard convention on defining polarization axes [29,31]. The complete

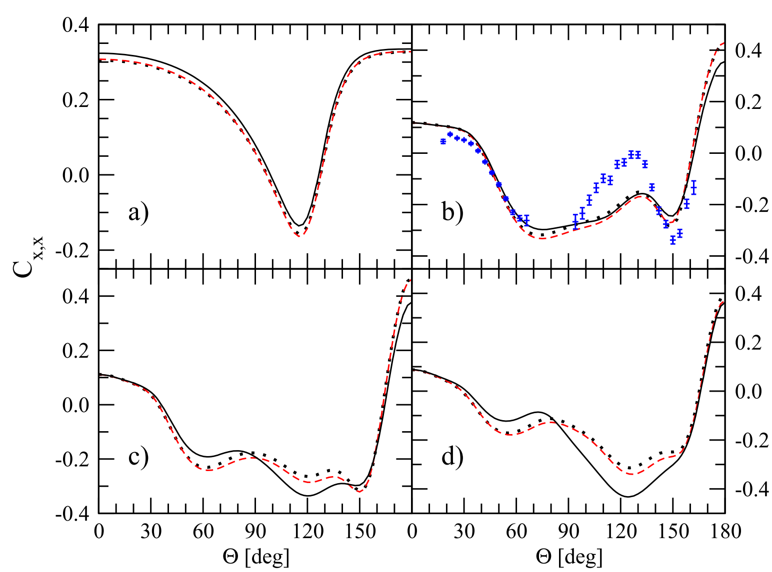

Fig. 1 The spin correlation coefficient $C_{x,x}$ for neutron-deuteron (nd) scattering at four laboratory energies of the incoming nucleon: a) E = 10 MeV, b) E = 135 MeV, c) E = 190 MeV, and d) E = 250 MeV. The predictions based on the 2N SMS N^{4}LO$^+$ interaction are represented by the black dotted curve. The red dashed curve shows predictions of the SMS model with 2N N^{4}LO$^+$ supplemented by the N^{2}LO 3NF and the black solid curve represents the N^{4}LO$^+$ + N^{2}LO 3NF + short-range N^{4}LO 3NF results

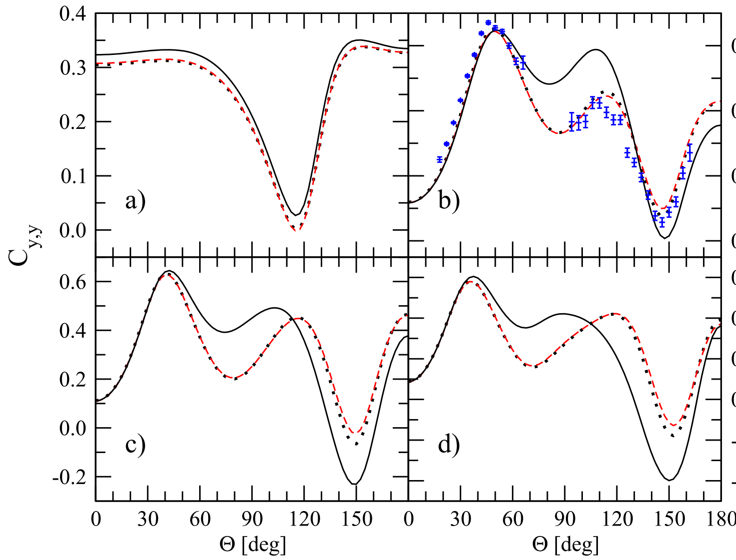

Fig. 2 The same as in Fig. 1 but for the $C_{y,y}$ coefficient

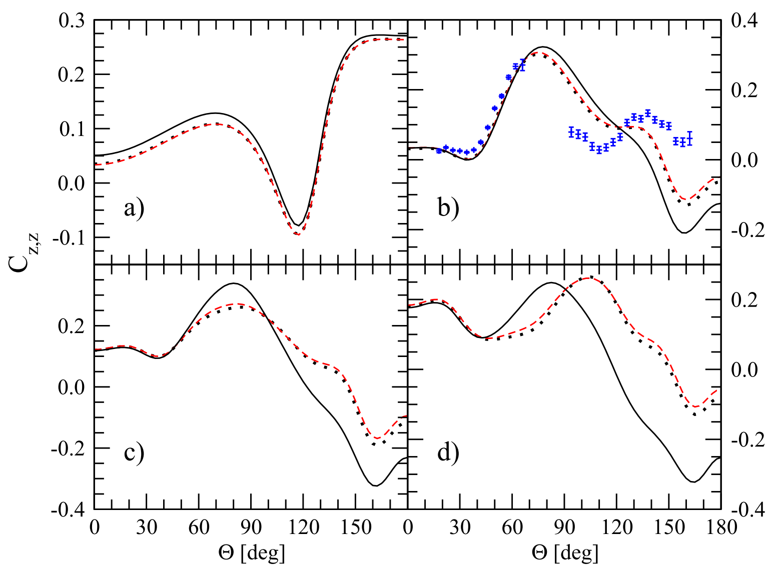

Fig. 3 The same as in Fig. 1 but for the $C_{z,z}$ coefficient

set of spin correlation coefficients is shown in Figs. 1, 2, 3, 4, 5, 6, 7, 8, 9, 10, 11, 12, and 13 as a function of the centre-of-mass scattering angle θ. In each figure we show predictions at four neutron beam laboratory energies: E = 10 MeV (left top), E = 135 MeV (right top), E = 190 MeV (left bottom) and E = 250 MeV (right bottom). Note that the two first energies are the ones used for fixing the $N^2LO + N^4LO$ 3NF parameters, thus strictly speaking among results based on N^4LO 3NF only the ones given in the bottom row are explicit predictions. All panels show calculations based on the 2N SMS N^4LO^+ only (black dotted curve), on the 2N SMS N^4LO^+ force combined with the complete N^2LO 3NF (red dashed curve), and on the later interaction supplemented by the N^4LO short-range 3NF (black solid curve). Finally, in some of the plots available data at E = 135 MeV from the IUCF experiment [23] are shown.

Even a quick look at the figures reveals that inclusion of the N^4LO short-range 3NF in most cases changes the predictions significantly. This is observed already at the lowest energy E = 10 MeV, where introducing

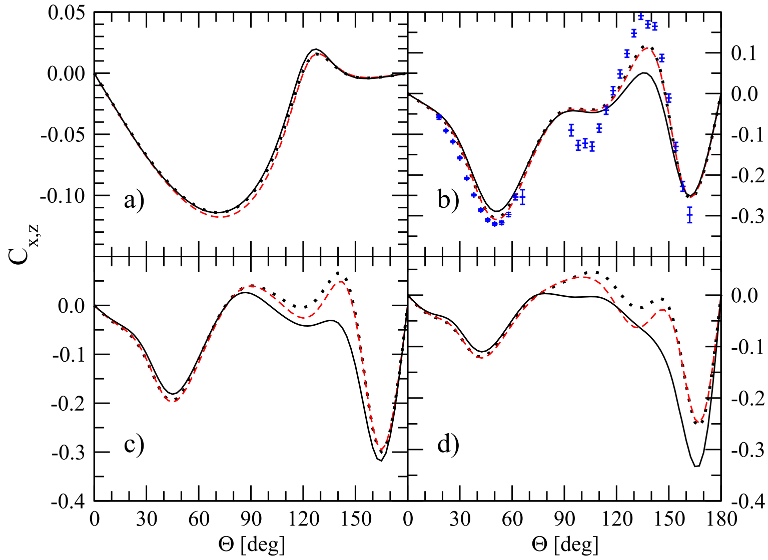

Fig. 4 The same as in Fig. 1 but for the $C_{x,z}$ coefficient

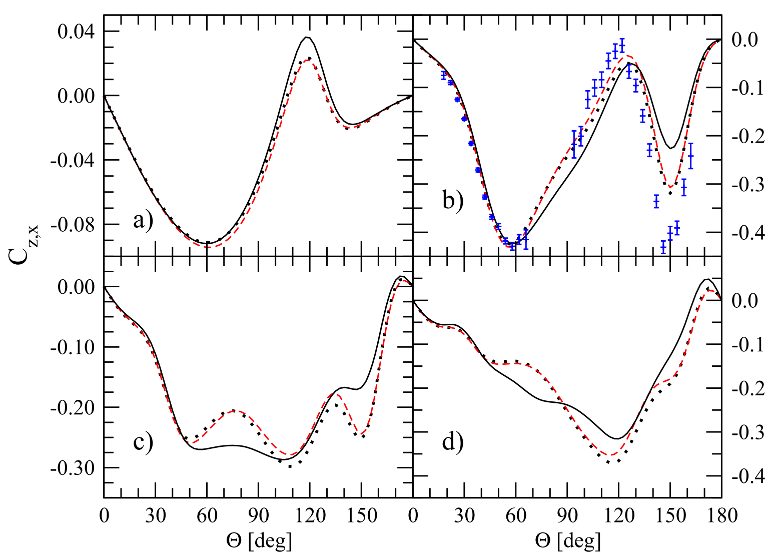

Fig. 5 The same as in Fig. 1 but for the $C_{z,x}$ coefficient

the N^{4}LO shifts the prediction by a few percent. To be more quantitative let us define the relative difference

$$\Delta(C_{\alpha,\beta}, \theta) \equiv \frac{C_{\alpha,\beta}^{full} - C_{\alpha,\beta}}{0.5(C_{\alpha,\beta}^{full} + C_{\alpha,\beta})}, \quad (5)$$

with $C_{\alpha,\beta}^{full}$ being the spin correlation coefficient with neutron and deuteron spin polarizations denoted by α and β obtained with inclusion of the 3NF N^{4}LO terms. The $C_{\alpha,\beta}$ values are calculated only with the N^{2}LO 3NF. Obviously both spin correlation coefficients entering formula (5) have to be taken at the same scattering angle θ.

Exemplary values of $\Delta(C_{\alpha,\beta})$ at E $= 10$ MeV are: $\Delta(C_{y,y}, 60^\circ) = 6.05\%$ and $\Delta(C_{y,y}, 115^\circ) \approx 220\%$ with the latter angle chosen at the minimum of the $C_{y,y}$ where its value is close to zero, what explains big value of $\Delta(C_{y,y}, 115^\circ)$. Strong influence of the N^{4}LO 3NF is also seen for $C_{xy,x}$ in Fig. 7 ($\Delta(C_{xy,x}, 80^\circ) = 116\%$) or $C_{zz,y}$ in Fig. 13 ($\Delta(C_{zz,y}, 115^\circ) = -36\%$). It is also worth noting that the spin correlation coefficient at

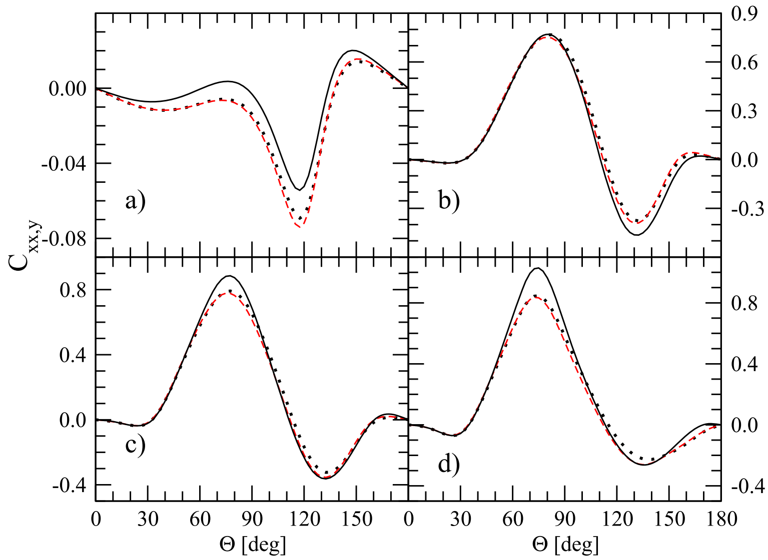

Fig. 6 The same as in Fig. 1 but for the $C_{xx,y}$ coefficient

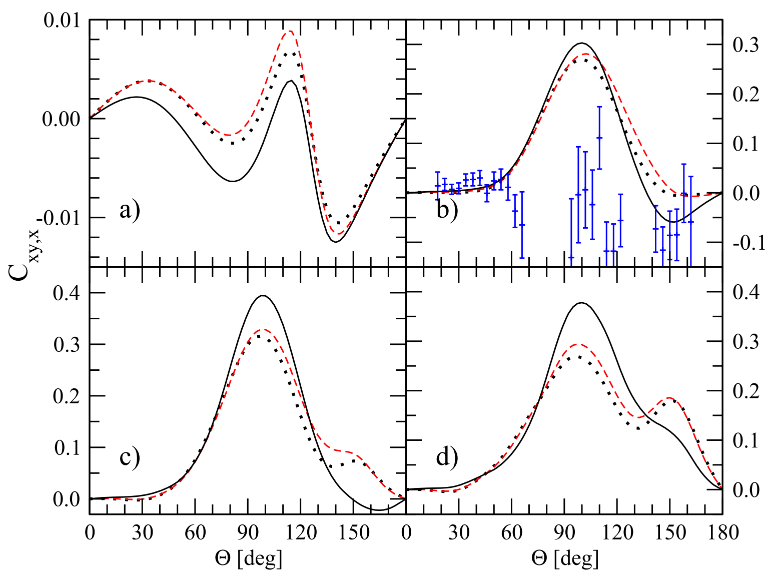

Fig. 7 The same as in Fig. 1 but for the $C_{xy,x}$ coefficient

E = 10 MeV, in the case of the deuteron tensor polarization, takes on small values, what makes it currently useless in experimental tests.

At E = 135 MeV the role of the N^{4}LO short-range 3NF remains significant for $C_{y,y}$ (Fig. 2) at the central scattering angles, $C_{x,z}$ ($C_{z,x}$) at the maximum (minimum) at backward scattering angles (Figs. 4 and 5), and for $C_{yz,z}$ (Fig. 12) above $\theta > 90°$. For these observables the relative difference reaches $\Delta(C_{y,y}, 90°) = 41\%$, $\Delta(C_{z,x}, 150°) = 30\%$, and $\Delta(C_{yz,z}, 130°) = 167\%$. As for the E = 10 MeV, at E = 135 MeV the chiral N^{2}LO is practically meaningless, and only slightly modifies predictions based on pure 2N force. Comparison with the data reveals clear discrepancies for many of the spin correlation coefficients. These discrepancies are already seen for predictions based on the 2N foce only or on the 2N force combined with N^{2}LO 3N interaction. Inclusion of the short-range N^{4}LO components of the 3NF either does not change the picture, as e.g. for $C_{x,x}$ (Fig. 1), $C_{z,z}$ (Fig. 3), or $C_{xy,x}$ (Fig. 7), or makes the discrepancy even worse, see e.g. $C_{y,y}$ (Fig 2) and $C_{zz,y}$ (Fig. 13).

The situation at E = 190 MeV resembles that at E = 135 MeV. The N^{4}LO terms are important for most of the coefficients and scattering angle's ranges. For $C_{y,y}$ (Fig. 2) $\Delta(C_{y,y}, 80°) = 65\%$, for $C_{yz,x}$ (Fig. 11)

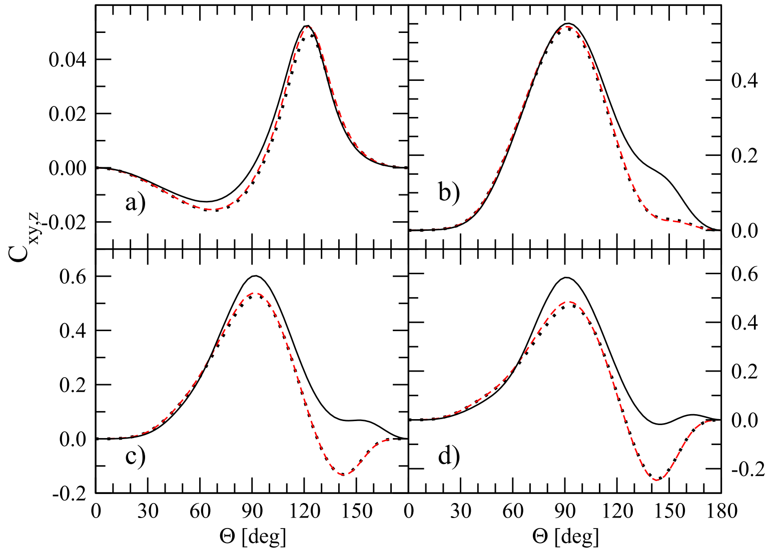

Fig. 8 The same as in Fig. 1 but for the $C_{xy,z}$ coefficient

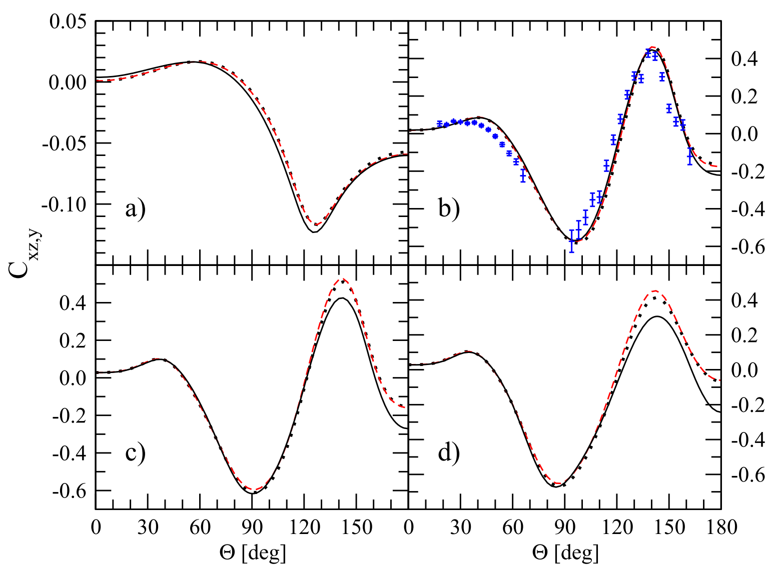

Fig. 9 The same as in Fig. 1 but for the $C_{xz,y}$ coefficient

$\Delta(C_{yz,x}, 125°) = -92\%$, and for $C_{yz,z}$ (Fig. 12) $\Delta(C_{yz,z}, 130°) = 182\%$. Only for $C_{x,x}$ (Fig. 1), $C_{xx,y}$ (Fig. 6), and $C_{x,zy}$ (Fig. 9) the N^4LO components of the 3NF have little impact on the results.

Also at the highest considered energy, E = 250 MeV, we do not observe many changes. In most cases the angular dependence of $C_{\alpha,\beta}$ is similar to that for E = 190 MeV. The N^4LO 3NF yields more or less similar Δ's leading to $\Delta(C_{y,y}, 80°) = 66\%$, $\Delta(C_{yz,x}, 125°) = -79\%$, and $\Delta(C_{yz,z}, 130°) = 113\%$ for the same cases as shown above for E = 190 MeV.

4 Conclusions

We have presented a complete set of the spin correlation coefficients for the neutron-deuteron elastic scattering in the energy range 10–250 MeV. That choice was partly dictated by the planned future experiments. Specifically, we investigated the significance of the whole set of short-range components of the N^4LO three-nucleon interaction [12–14]. That force has been combined with the SMS N^4LO^+ two-nucleon [10] and the N^2LO [7]

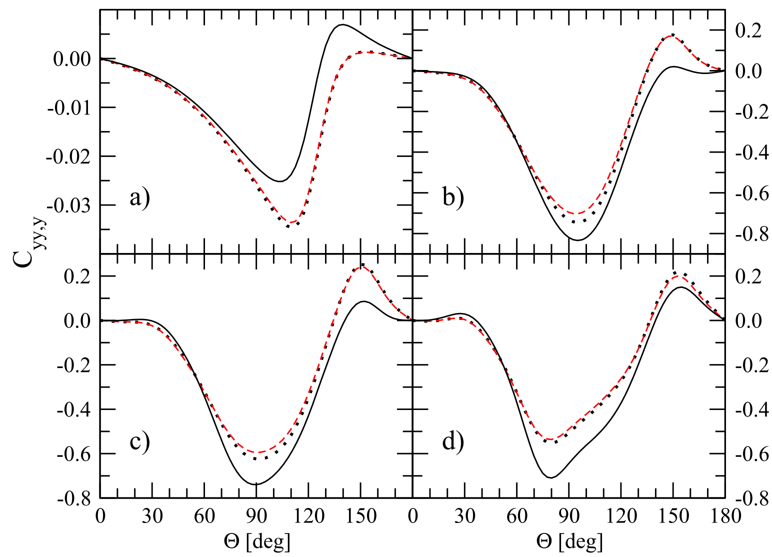

Fig. 10 The same as in Fig. 1 but for the $C_{yy,y}$ coefficient

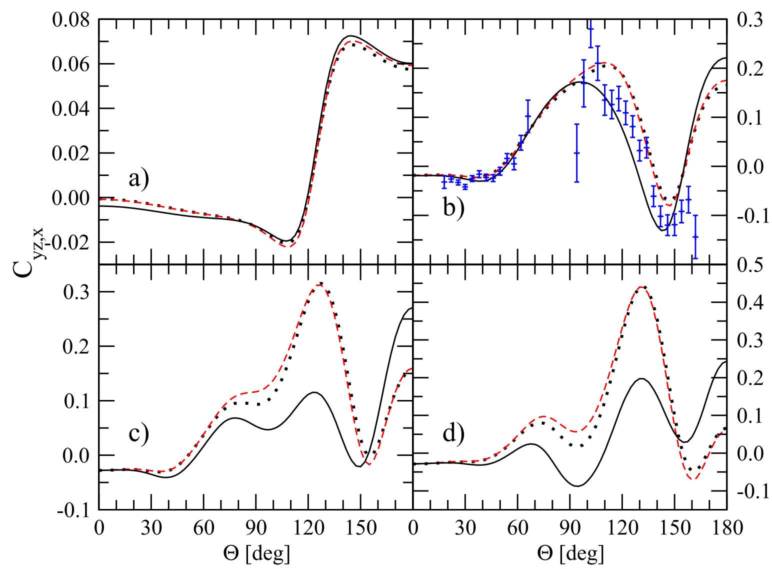

Fig. 11 The same as in Fig. 1 but for the $C_{yz,x}$ coefficient

three-nucleon potentials. The 13 strength parameters of the 3NF were found by performing a χ^2-minimization to three-nucleon data. It was possible thanks to the use of the emulator of Faddeev equations proposed in our earlier works [26–28].

We found that the included N^{4}LO 3NF has a significant impact on the predicted spin correlation coefficients for most of them. Depending on the reaction energy, the scattering angle and specific choice of the polarization observable, the N^{4}LO 3NF changes the magnitude of some spin correlation coefficients even by several dozen percent. In general, the $C_{yz,z}$ and $C_{yz,x}$ at higher energies seem to be the most sensitive to that new 3NF components and thus the most interesting coefficients to be compared with future experimental data. On the other hand, the N^{4}LO 3NF contributions have only tiny effect on the $C_{xz,y}$ and $C_{xx,y}$ spin correlation coefficients.

A comparison with the available data [23] at E = 135 MeV reveals two cases. For some observables, like $C_{x,x}$ or $C_{z,z}$, there is no improvement in data description. However, we found also coefficients, e.g. $C_{y,y}$ and $C_{zz,y}$ for which the N^{4}LO short-range 3NF moves theoretical predictions away from the data.

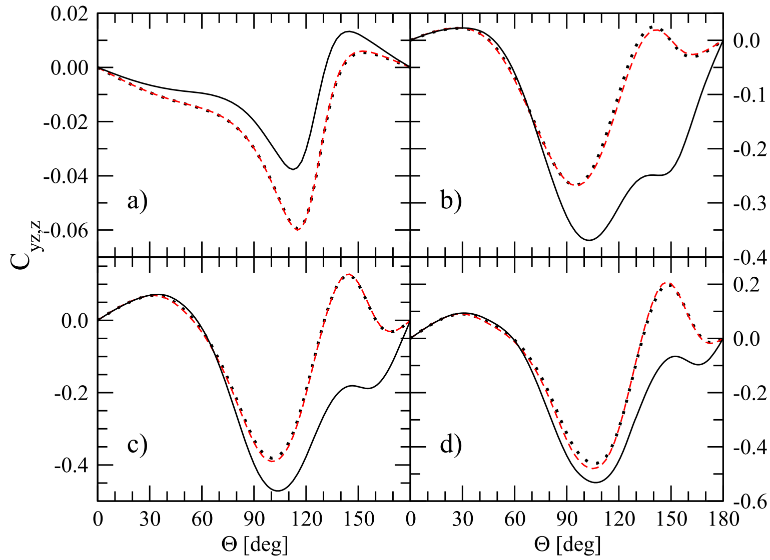

Fig. 12 The same as in Fig. 1 but for the $C_{yz,z}$ coefficient

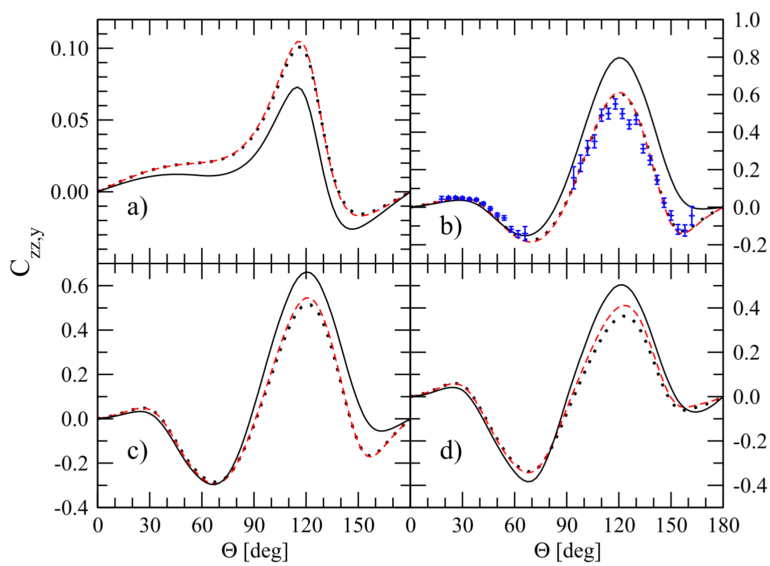

Fig. 13 The same as in Fig. 1 but for the $C_{zz,y}$ coefficient

Due to the missing N^{3}LO 3NF components our study should be regarded as preliminary. Results with such an unexpectedly big role of N^{4}LO 3NF indicate that it is necessary to include first the three-body force at N^{3}LO in the analysis. Note that this will require re-adjusting the values of the free parameters c_D, c_E in the N^{2}LO and c_i in the N^{4}LO 3NF. There are no new free parameters of 3NF at N^{3}LO [32,33]. The magnitude of the observed discrepancies between the data and the current predictions is one more argument for an important role of the N^{3}LO 3NF contributions. The work on derivation and partial wave decomposition of the N^{3}LO 3NF is ongoing.

Acknowledgements This research was supported in part by the Excellence Initiative – Research University Program at the Jagiellonian University in Kraków. The numerical calculations were performed on the supercomputer cluster of the JSC, Jülich, Germany.

Open Access This article is licensed under a Creative Commons Attribution 4.0 International License, which permits use, sharing, adaptation, distribution and reproduction in any medium or format, as long as you give appropriate credit to the original author(s) and the source, provide a link to the Creative Commons licence, and indicate if changes were made. The images or other third party material in this article are included in the article's Creative Commons licence, unless indicated otherwise in a credit line to the material. If material is not included in the article's Creative Commons licence and your intended use is not permitted by statutory regulation or exceeds the permitted use, you will need to obtain permission directly from the copyright holder. To view a copy of this licence, visit http://creativecommons.org/licenses/by/4.0/.

Author Contributions All authors (R.S., H.W., J.G.) contributed to the manuscript by doing research and preparing manuscript.

Data Availability No datasets were generated or analysed during the current study.

Declarations

Conflict of interest The authors declare no competing interests.

References

1. R.B. Wiringa, V.G.J. Stoks, R. Schiavilla, Accurate nucleon-nucleon potential with charge-independence breaking. Phys. Rev. C **51**, 38–51 (1995). https://doi.org/10.1103/PhysRevC.51.38
2. R. Machleidt, High-precision, charge-dependent Bonn nucleon–nucleon potential. Phys. Rev. C **63**, 024001 (2001). https://doi.org/10.1103/PhysRevC.63.024001
3. D.R. Entem, R. Machleidt, Accurate charge dependent nucleon nucleon potential at fourth order of chiral perturbation theory. Phys. Rev. C **68**, 041001 (2003). https://doi.org/10.1103/PhysRevC.68.041001
4. D.R. Entem, R. Machleidt, Y. Nosyk, High-quality two-nucleon potentials up to fifth order of the chiral expansion. Phys. Rev. C **96**, 024004 (2017). https://doi.org/10.1103/PhysRevC.96.024004
5. E. Epelbaoum, W. Glöckle, U.-G. Meißner, Nuclear forces from chiral lagrangians using the method of unitary transformation (i): formalism. Nucl. Phys. A **637**(1), 107–134 (1998). https://doi.org/10.1016/S0375-9474(98)00220-6
6. E. Epelbaum, W. Glöckle, U.-G. Meißner, Nuclear forces from chiral lagrangians using the method of unitary transformation ii: The two-nucleon system. Nucl. Phys. A **671**(1), 295–331 (2000). https://doi.org/10.1016/S0375-9474(99)00821-0
7. E. Epelbaum, A. Nogga, W. Glöckle, H. Kamada, U.-G. Meißner, H. Witała, Three-nucleon forces from chiral effective field theory. Phys. Rev. C **66**, 064001 (2002). https://doi.org/10.1103/PhysRevC.66.064001
8. E. Epelbaum, H. Krebs, U.-G. Meißner, Improved chiral nucleon-nucleon potential up to next-to-next-to-next-to-leading order. Eur. Phys. J. A **51**, 53 (2015). https://doi.org/10.1140/epja/i2015-15053-8
9. E. Epelbaum, H. Krebs, U.-G. Meißner, Precision nucleon–nucleon potential at fifth order in the chiral expansion. Phys. Rev. Lett. **115**, 122301 (2015). https://doi.org/10.1103/PhysRevLett.115.122301
10. P. Reinert, H. Krebs, E. Epelbaum, H. Krebs, Semilocal momentum-space regularized chiral two-nucleon potentials up to fifth order. Eur. Phys. J. A **54**, 86 (2018). https://doi.org/10.1140/epja/i2018-12516-4
11. M. Piarulli, L. Girlanda, R. Schiavilla, A. Kievsky, A. Lovato, L.E. Marcucci, S.C. Pieper, M. Viviani, R.B. Wiringa, Local chiral potentials with Δ-intermediate states and the structure of light nuclei. Phys. Rev. C **94**, 054007 (2016). https://doi.org/10.1103/PhysRevC.94.054007
12. L. Girlanda, A. Kievsky, M. Viviani, Subleading contributions to the three-nucleon contact interaction. Phys. Rev. C **84**, 014001 (2011). https://doi.org/10.1103/PhysRevC.84.014001
13. L. Girlanda, A. Kievsky, M. Viviani, L.E. Marcucci, Short-range three-nucleon interaction from $a = 3$ data and its hierarchical structure. Phys. Rev. C **99**, 054003 (2019). https://doi.org/10.1103/PhysRevC.99.054003
14. L. Girlanda, A. Kievsky, M. Viviani, Erratum: Subleading contributions to the three-nucleon contact interaction [Phys. Rev. C 84, 014001 (2011)]. Phys. Rev. C **102**, 019903 (2020). https://doi.org/10.1103/PhysRevC.102.019903
15. L. Girlanda, A. Kievsky, L.E. Marcucci, M. Viviani, Unitary ambiguity of nn contact interactions and the $3n$ force. Phys. Rev. C **102**, 064003 (2020). https://doi.org/10.1103/PhysRevC.102.064003
16. L. Girlanda, E. Filandri, A. Kievsky, L.E. Marcucci, M. Viviani, Effect of the n3lo three-nucleon contact interaction on p-d scattering observables. Phys. Rev. C **107**, 061001 (2023). https://doi.org/10.1103/PhysRevC.107.L061001
17. S. Kistryn, E. Stephan, A. Biegun, K. Bodek, A. Deltuva, E. Epelbaum, K. Ermisch, W. Glöckle, J. Golak, N. Kalantar-Nayestanaki, H. Kamada, M. Kiś, B. Kłos, A. Kozela, J. Kuroś-Żołnierczuk, M. Mahjour-Shafiei, U.-G. Meißner, A. Micherdzińska, A. Nogga, P.U. Sauer, R. Skibiński, R. Sworst, H. Witała, J. Zejma, W. Zipper, Systematic study of three-nucleon force effects in the cross section of the deuteron-proton breakup at 130 mev. Phys. Rev. C **72**, 044006 (2005). https://doi.org/10.1103/PhysRevC.72.044006
18. H. Tavakoli-Zaniani, M. Eslami-Kalantari, H.R. Amir-Ahmadi, M.T. Bayat, A. Deltuva, J. Golak, N. Kalantar-Nayestanaki, S. Kistryn, A. Kozela, H. Mardanpour, J.G. Messchendorp, M. Mohammadi-Dadkan, A. Ramazani-Moghaddam-Arani, R. Ramazani-Sharifabadi, R. Skibiński, E. Stephan, H. Witała, A comprehensive analysis of differential cross sections and analyzing powers in the proton-deuteron break-up channel at 135 mev. Eur. Phys. J. A **57**, 58 (2021). https://doi.org/10.1140/epja/s10050-021-00358-2
19. W. Parol, A. Kozela, K. Bodek, A. Deltuva, M. Eslami-Kalantari, J. Golak, N. Kalantar-Nayestanaki, G. Khatri, S. Kistryn, B. Kłos, J. Kuboś, P. Kulessa, A. Łobejko, A. Magiera, H. Mardanpour, J.G. Messchendorp, I. Mazumdar, R. Skibiński, I. Skwira-Chalot, E. Stephan, A. Ramazani-Moghaddam-Arani, D. Rozpędzik, A. Wilczek, H. Witała, B. Włoch, A. Wrońska, J. Zejma, Measurement of differential cross sections for the deuteron-proton breakup reaction at 160 mev. Phys. Rev. C **102**, 054002 (2020). https://doi.org/10.1103/PhysRevC.102.054002
20. K. Sekiguchi, H. Sakai, H. Witała, W. Glöckle, J. Golak, M. Hatano, H. Kamada, H. Kato, Y. Maeda, J. Nishikawa, A. Nogga, T. Ohnishi, H. Okamura, N. Sakamoto, S. Sakoda, Y. Satou, K. Suda, A. Tamii, T. Uesaka, T. Wakasa, K. Yako, Complete set of precise deuteron analyzing powers at intermediate energies: comparison with modern nuclear force predictions. Phys. Rev. C **65**, 034003 (2002). https://doi.org/10.1103/PhysRevC.65.034003

21. K. Sekiguchi, H. Sakai, H. Witała, W. Glöckle, J. Golak, K. Hatanaka, M. Hatano, K. Itoh, H. Kamada, H. Kuboki, Y. Maeda, A. Nogga, H. Okamura, T. Saito, N. Sakamoto, Y. Sakemi, M. Sasano, Y. Shimizu, K. Suda, A. Tamii, T. Uesaka, T. Wakasa, K. Yako, Resolving the discrepancy of 135 MeV *pd* elastic scattering cross sections and relativistic effects. Phys. Rev. Lett. **95**, 162301 (2005). https://doi.org/10.1103/PhysRevLett.95.162301
22. K. Sekiguchi, H. Witała, T. Akieda, D. Eto, H. Kon, Y. Wada, A. Watanabe, S. Chebotaryov, M. Dozono, J. Golak, H. Kamada, S. Kawakami, Y. Kubota, Y. Maeda, K. Miki, E. Milman, A. Ohkura, H. Sakai, S. Sakaguchi, N. Sakamoto, M. Sasano, Y. Shindo, R. Skibiński, H. Suzuki, M. Tabata, T. Uesaka, T. Wakasa, K. Yako, T. Yamamoto, Y. Yanagisawa, J. Yasuda, Complete set of deuteron analyzing powers from $\mathbf{d}p$ elastic scattering at 190 mev/nucleon. Phys. Rev. C **96**, 064001 (2017). https://doi.org/10.1103/PhysRevC.96.064001
23. B. Przewoski, H.O. Meyer, J.T. Balewski, W.W. Daehnick, J. Doskow, W. Haeberli, R. Ibald, B. Lorentz, R.E. Pollock, P.V. Pancella, F. Rathmann, T. Rinckel, S.K. Saha, B. Schwartz, P. Thörngren-Engblom, A. Wellinghausen, T.J. Whitaker, T. Wise, Analyzing powers and spin correlation coefficients for $p + d$ elastic scattering at 135 and 200 mev. Phys. Rev. C **74**, 064003 (2006). https://doi.org/10.1103/PhysRevC.74.064003
24. Y. Saito, A. Watanabe, D. Takahashi, D. Miura, H. Otsu, H. Sakai, H. Nishibata, H. Sugahara, K. Aradono, K. Tateishi, K. Hirasawa, K. Sekiguchi, K. Suzuki, N. Sakamoto, S. Sakaguchi, T. Kajihara, T. Wakui, T. Matsui, T. Uesaka, T. Wakasa, Y. Maruta, Preparation for spin correlation coefficients measurement in polarized deuteron-polarized proton scattering experiment, in *Book of Abstracts, 25th European Conference on Few-Body Problems in Physics, Mainz, Germany* (2023). pp. 60–61. Poster Session 99. https://indico.him.uni-mainz.de/event/150/book-of-abstracts.pdf
25. K. Sekiguchi, private communication
26. H. Witała, J. Golak, R. Skibiński, K. Topolnicki, Perturbative treatment of three-nucleon force contact terms in three-nucleon Faddeev equations. Few-Body Syst. **62**, 23 (2021). https://doi.org/10.1007/s00601-021-01607-2
27. H. Witała, J. Golak, R. Skibiński, Efficient emulator for solving three-nucleon continuum Faddeev equations with chiral three-nucleon force comprising any number of contact terms. Eur. Phys. J. A **57**, 241 (2021). https://doi.org/10.1140/epja/s10050-021-00555-z
28. H. Witała, J. Golak, R. Skibiński, Significance of chiral three-nucleon force contact terms for understanding of elastic nucleon-deuteron scattering. Phys. Rev. C **105**, 054004 (2022). https://doi.org/10.1103/PhysRevC.105.054004
29. W. Glöckle, H. Witała, D. Hüber, H. Kamada, J. Golak, The three-nucleon continuum: achievements, challenges and applications. Phys. Rep. **274**(3), 107–285 (1996). https://doi.org/10.1016/0370-1573(95)00085-2
30. D. Hüber, H. Kamada, H. Witała, W. Glöckle, How to include a three-nucleon force into Faddeev equations for the 3n continuum: a new form. Acta Phys. Pol. B **28**, 1677 (1997)
31. G.G. Ohlsen, Polarization transfer and spin correlation experiments in nuclear physics. Rep. Prog. Phys. **35**(2), 717 (1972). https://doi.org/10.1088/0034-4885/35/2/305
32. V. Bernard, E. Epelbaum, H. Krebs, U.-G. Meißner, Subleading contributions to the chiral three-nucleon force: long-range terms. Phys. Rev. C **77**, 064004 (2008). https://doi.org/10.1103/PhysRevC.77.064004
33. V. Bernard, E. Epelbaum, H. Krebs, U.-G. Meißner, Subleading contributions to the chiral three-nucleon force. ii. Short-range terms and relativistic corrections. Phys. Rev. C **84**, 054001 (2011). https://doi.org/10.1103/PhysRevC.84.054001

Publisher's Note Springer Nature remains neutral with regard to jurisdictional claims in published maps and institutional affiliations.